

SOME ASPECTS OF BARYOGENESIS AND LEPTON NUMBER VIOLATION

W. BUCHMULLER
*Deutsches Elektronen-Synchrotron DESY
Notkestr. 85, D-22607 Hamburg, Germany*

Abstract. The cosmological baryon asymmetry is closely related to neutrino properties due to the non-perturbative sphaleron processes in the high-temperature symmetric phase of the standard model. We review some aspects of this connection with emphasis on cosmological bounds on neutrino masses, leptogenesis and possible implications for dark matter.

Lectures at the NATO ASI 2000, Cascais, Portugal, 26 June - 7 July, 2000

1. Elements of baryogenesis

Particle physics unravels the structure of matter at short distances. The characteristic energy scales of the different layers of structure are of order 1 eV, the binding energy of atoms, 1 MeV, the binding energy of nuclei, and 100 GeV, the typical collision energy of quarks and leptons in present day high-energy colliders. Knowledge of the laws of nature which govern the interactions of elementary particles at these energies allows us to calculate the properties of a plasma of particles at the corresponding temperatures. Extrapolating the observed Hubble expansion of the universe back to early times one concludes that such temperatures must have been realized in the early stages of the evolution of the universe.

At a temperature $T \sim 1$ eV electrons and nuclei combined to neutral atoms and the universe became transparent to photons. The observation and recent detailed investigation of the corresponding cosmic microwave background [1] is the basis of early-universe cosmology. The second main success is the prediction of the abundances of the light elements, D, ^3He , ^4He and ^7Li based on the properties of the lightest baryons, protons and neutrons. The light elements were formed at a temperature $T \sim 1$ MeV. Agreement between theory and observation is obtained for a certain range of the parameter η , the ratio of baryon density and photon density [2],

$$\eta = \frac{n_B}{n_\gamma} = (1.5 - 6.3) \times 10^{-10} , \quad (1)$$

where the present number density of photons is $n_\gamma \sim 400/\text{cm}^3$. Since no significant amount of antimatter is observed in the universe, the baryon density is equal to the cosmological baryon asymmetry, $n_B \simeq n_B - n_{\bar{B}}$.

The formation of the cosmological baryon asymmetry, i.e., the origin of the observed matter density today, can be understood in terms of the properties of quarks and leptons, the building blocks of the standard model which describes their interactions at energies of order 100 GeV and beyond. There are three families of left-handed and right-handed up-type and down-type quarks with baryon number $B = 1/3$ and lepton number $L = 0$, and three families of left-handed neutrinos and left- and right-handed electron-type leptons with $B = 0$ and $L = 1$,

$$q_{Li} = \begin{pmatrix} u_{Li} \\ d_{Li} \end{pmatrix}, \quad u_{Ri}, \quad d_{Ri}, \quad l_{Li} = \begin{pmatrix} \nu_{Li} \\ e_{Li} \end{pmatrix}, \quad e_{Ri}, \quad i = 1 \dots 3. \quad (2)$$

Some of their interactions are not invariant under charge conjugation (C) and the combined charge conjugation and parity (CP) transformation [3].

A matter-antimatter asymmetry can be dynamically generated in an expanding universe if the particle interactions and the cosmological evolution satisfy Sakharov's conditions [4], i.e.,

- baryon number violation
- C and CP violation
- deviation from thermal equilibrium .

At present there are a number of viable scenarios for baryogenesis. They can be classified according to the different ways in which Sakharov's conditions are realized. Already in the standard model C and CP are not conserved. Also B and L are violated by instanton processes [5]. In grand unified theories B and L are broken by the interactions of heavy gauge bosons and leptoquarks. This is the basis of the classical GUT baryogenesis [6]. Analogously, the L violating decays of heavy Majorana neutrinos lead to leptogenesis [7]. In supersymmetric theories the existence of approximately flat directions in the scalar potential provides new possibilities. Coherent oscillations of scalar fields may then generate large asymmetries [8].

The crucial departure from thermal equilibrium can also be realized in several ways. One possibility is a sufficiently strong first-order electroweak phase transition [9]. In this case CP violating interactions of the standard model or its supersymmetric extension could in principle generate the observed baryon asymmetry. However, due to the rather large lower bound on the Higgs boson mass of about 115 GeV, which is imposed by the LEP experiments, this interesting possibility is now restricted to a very small range of parameters in the supersymmetric standard model. In the case of the Affleck-Dine scenario the baryon asymmetry is generated at the end of an inflationary period as a coherent effect of scalar fields which leads

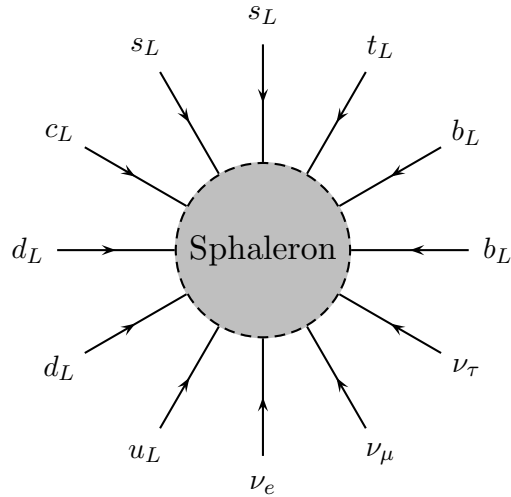


Figure 1. One of the 12-fermion processes which are in thermal equilibrium in the high-temperature phase of the standard model.

to an asymmetry between quarks and antiquarks after reheating [10]. For the classical GUT baryogenesis and for leptogenesis the departure from thermal equilibrium is due to the deviation of the number density of the decaying heavy particles from the equilibrium number density. How strong this deviation from thermal equilibrium is depends on the lifetime of the decaying heavy particles and the cosmological evolution. Further scenarios for baryogenesis are described in [11].

The theory of baryogenesis involves non-perturbative aspects of quantum field theory and also non-equilibrium statistical field theory, in particular the theory of phase transitions and kinetic theory. A crucial ingredient is also the connection between baryon number and lepton number in the high-temperature, symmetric phase of the standard model. Due to the chiral nature of the weak interactions B and L are not conserved. At zero temperature this has no observable effect due to the smallness of the weak coupling. However, as the temperature approaches the critical temperature T_{EW} of the electroweak transition, B and L violating processes come into thermal equilibrium [12].

The rate of these processes is related to the free energy of sphaleron-type field configurations which carry topological charge. In the standard model they lead to an effective interaction of all left-handed quarks and

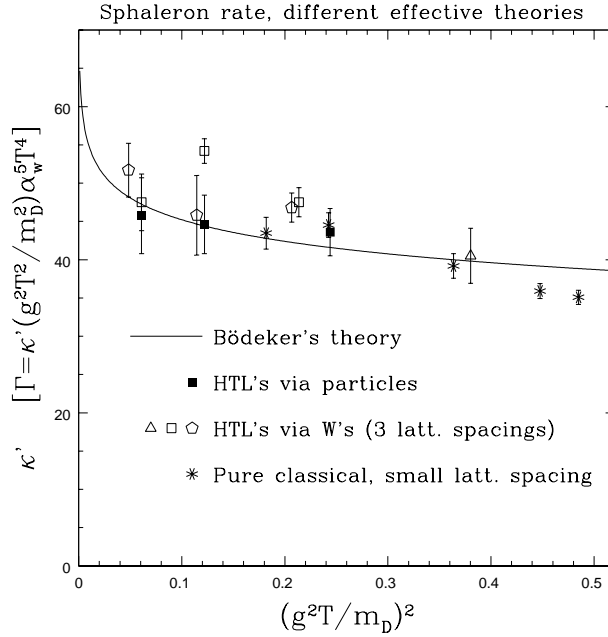


Figure 2. Sphaleron rate in Bödeker's effective theory, two lattice implementations of HTL effective theory, and pure lattice theory interpreted as HTL effective theory [14].

leptons [5] (cf. fig. 1),

$$O_{B+L} = \prod_i (q_{Li} q_{Li} q_{Li} l_{Li}) , \quad (3)$$

which violates baryon and lepton number by three units,

$$\Delta B = \Delta L = 3 . \quad (4)$$

The evaluation of the sphaleron rate in the symmetric high-temperature phase is a complicated problem. A clear physical picture has been obtained in Bödeker's effective theory [13] according to which low-frequency gauge field fluctuations satisfy the equation of motion

$$\mathbf{D} \times \mathbf{B} = \sigma \mathbf{E} - \zeta . \quad (5)$$

Here ζ is Gaussian noise, i.e., a random vector field with variance

$$\langle \zeta_i(t, \mathbf{x}) \zeta_j(t', \mathbf{x}') \rangle = 2\sigma \delta_{ij} \delta(t - t') \delta(\mathbf{x} - \mathbf{x}') , \quad (6)$$

and σ is a non-abelian conductivity. The sphaleron rate can then be written as [14],

$$\Gamma \simeq (14.0 \pm 0.3) \frac{1}{\sigma} (\alpha_w T)^5 . \quad (7)$$

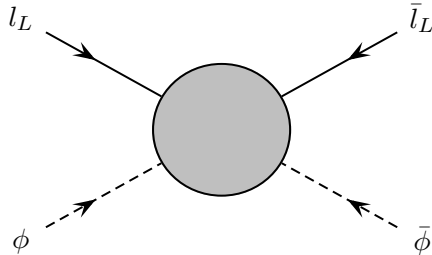


Figure 3. Effective lepton number violating interaction.

A comparison with two lattice simulations is shown in fig. 2. From this one derives that B and L violating processes are in thermal equilibrium for temperatures in the range

$$T_{EW} \sim 100 \text{ GeV} < T < T_{SPH} \sim 10^{12} \text{ GeV} . \quad (8)$$

Sphaleron processes have a profound effect on the generation of the cosmological baryon asymmetry, in particular in connection with lepton number violating interactions between lepton and Higgs fields,

$$\mathcal{L}_{\Delta L=2} = \frac{1}{2} f_{ij} l_{Li}^T \varphi C l_{Lj} \varphi + \text{h.c.} . \quad (9)$$

Such an interaction arises in particular from the exchange of heavy Majorana neutrinos (cf. fig. 3). In the Higgs phase of the standard model, where the Higgs field acquires a vacuum expectation value, it gives rise to Majorana masses of the light neutrinos ν_e , ν_μ and ν_τ .

Eq. (4) suggests that any $B + L$ asymmetry generated before the electroweak phase transition, i.e., at temperatures $T > T_{EW}$, will be washed out. However, since only left-handed fields couple to sphalerons, a non-zero value of $B + L$ can persist in the high-temperature, symmetric phase if there exists a non-vanishing $B - L$ asymmetry. An analysis of the chemical potentials of all particle species in the high-temperature phase yields a relation between the baryon asymmetry $Y_B = (n_B - n_{\bar{B}})/s$, where s is the entropy density, and the corresponding $B - L$ and L asymmetries Y_{B-L} and Y_L , respectively [15],

$$Y_B = a Y_{B-L} = \frac{a}{a-1} Y_L . \quad (10)$$

The number a depends on the other processes which are in thermal equilibrium. If these are all standard model interactions one has $a = 28/79$. If instead of the Yukawa interactions of the right-handed electron the $\Delta L = 2$ interactions (9) are in equilibrium one finds $a = -2/3$ [16].

The interplay between the sphaleron processes (fig. 1) and the lepton number violating processes (fig. 3) leads to an intriguing relation between neutrino properties and the cosmological baryon asymmetry. The decay of heavy Majorana neutrinos can quantitatively account for the observed asymmetry.

2. Heavy particle decays in a thermal bath

Let us now consider the simplest possibility for a departure from thermal equilibrium, the decay of heavy, weakly interacting particles in a thermal bath. To be specific, we choose the heavy particle to be a Majorana neutrino $N = N^c$ which can decay into a lepton Higgs pair $l\phi$ and also into the CP conjugate state $\bar{l}\bar{\phi}$

$$N \rightarrow l\phi, \quad N \rightarrow \bar{l}\bar{\phi}. \quad (11)$$

In the case of CP violating couplings a lepton asymmetry can be generated in the decays of the heavy neutrinos N which is then partially transformed into a baryon asymmetry by sphaleron processes [7]. Compared to other scenarios of baryogenesis this leptogenesis mechanism has the advantage that, at least in principle, the resulting baryon asymmetry is entirely determined by neutrino properties.

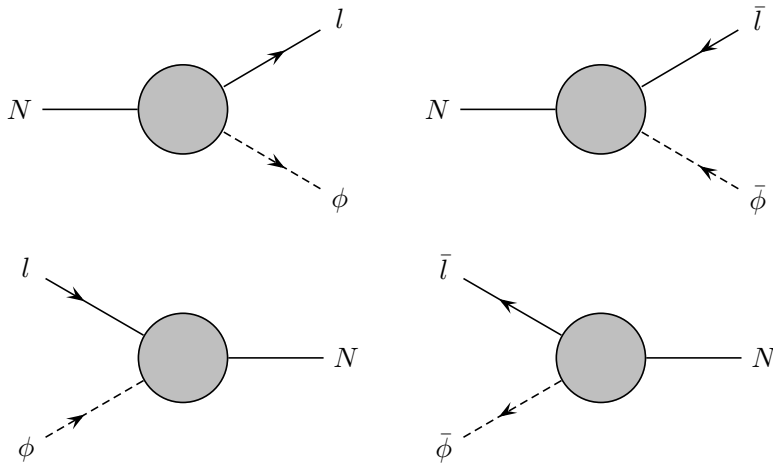


Figure 4. $\Delta L = 1$ processes: decays and inverse decays of a heavy Majorana neutrino.

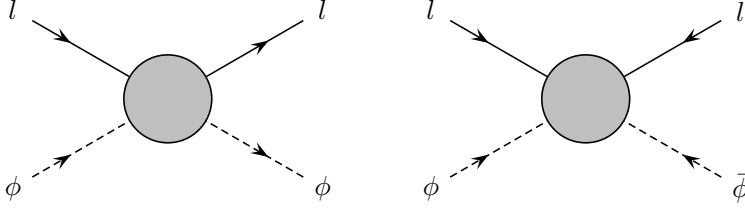


Figure 5. $\Delta L = 0$ and $\Delta L = 2$ lepton Higgs processes.

2.1. BOLTZMANN EQUATIONS

The generation of a baryon asymmetry is an out-of-equilibrium process which is generally treated by means of Boltzmann equations. A detailed discussion of the basic ideas and some of the subtleties has been given in [17]. The main processes in the thermal bath are the decays and the inverse decays of the heavy neutrinos (cf. fig. 4), and the lepton number conserving ($\Delta L = 0$) and violating ($\Delta L = 2$) processes (cf. fig. 5). In addition there are other processes, in particular those involving the t-quark, which are also important in a quantitative analysis [18, 19]. A lepton asymmetry can be dynamically generated in an expanding universe if the partial decay widths of the heavy neutrino violate CP invariance, i.e.,

$$\Gamma(N \rightarrow l\phi) = \frac{1}{2}(1 + \epsilon)\Gamma, \quad \Gamma(N \rightarrow \bar{l}\bar{\phi}) = \frac{1}{2}(1 - \epsilon)\Gamma. \quad (12)$$

Here Γ is the total decay width, and the parameter $\epsilon \ll 1$ measures the amount of CP violation.

The Boltzmann equations for the number densities of heavy neutrinos (n_N), leptons (n_l) and antileptons ($n_{\bar{l}}$) corresponding to the processes in figs. 4 and 5 are given by

$$\begin{aligned} \frac{dn_N}{dt} + 3Hn_N &= -\gamma(N \rightarrow l\phi) + \gamma(l\phi \rightarrow N) \\ &\quad -\gamma(N \rightarrow \bar{l}\bar{\phi}) + \gamma(\bar{l}\bar{\phi} \rightarrow N), \end{aligned} \quad (13)$$

$$\begin{aligned} \frac{dn_l}{dt} + 3Hn_l &= \gamma(N \rightarrow l\phi) - \gamma(l\phi \rightarrow N) \\ &\quad + \gamma(\bar{l}\bar{\phi} \rightarrow l\phi) - \gamma(l\phi \rightarrow \bar{l}\bar{\phi}), \end{aligned} \quad (14)$$

$$\begin{aligned} \frac{dn_{\bar{l}}}{dt} + 3Hn_{\bar{l}} &= \gamma(N \rightarrow \bar{l}\bar{\phi}) - \gamma(\bar{l}\bar{\phi} \rightarrow N) \\ &\quad + \gamma(l\phi \rightarrow \bar{l}\bar{\phi}) - \gamma(\bar{l}\bar{\phi} \rightarrow l\phi), \end{aligned} \quad (15)$$

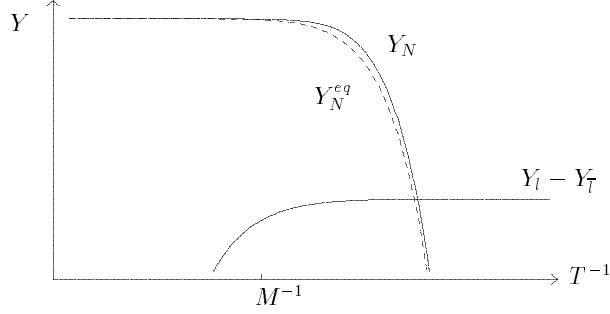


Figure 6. Time evolution of the number density to entropy density ratio. At $T \sim M$ the system gets out of equilibrium and an asymmetry is produced.

with the reaction rates

$$\gamma(N \rightarrow l\phi) = \int d\Phi_{123} f_N(p_1) |\mathcal{M}(N \rightarrow l\phi)|^2, \dots \quad (16)$$

$$\gamma(l\phi \rightarrow \bar{l}\bar{\phi}) = \int d\Phi_{1234} f_l(p_1) f_\phi(p_2) |\mathcal{M}'(l\phi \rightarrow \bar{l}\bar{\phi})|^2, \dots \quad (17)$$

Here H is the Hubble parameter, $d\Phi_{1\dots n}$ denotes the phase space integration over particles in initial and final states,

$$d\Phi_{1\dots n} = \frac{d^3 p_1}{(2\pi)^3 2E_1} \cdots \frac{d^3 p_n}{(2\pi)^3 2E_n} (2\pi)^4 \delta^4(p_1 + \dots - p_n), \quad (18)$$

and

$$f_i(p) = \exp(-\beta E_i(p)), \quad n_i(p) = g_i \int \frac{d^3 p}{(2\pi)^3} f_i(p), \quad (19)$$

are Boltzmann distribution and number density of particle $i = N, l, \phi$ at temperature $T = 1/\beta$, respectively. \mathcal{M} and \mathcal{M}' denote the scattering matrix elements of the indicated processes at zero temperature; the prime indicates that for the $2 \rightarrow 2$ processes the contribution of the intermediate resonance state has been subtracted. For simplicity we have used in eqs. (16) and (17) Boltzmann distributions rather than Bose-Einstein and Fermi-Dirac distributions, and we have also neglected the distribution functions in the final state, which is a good approximation for small number densities. Subtracting (15) from (14) yields the Boltzmann equation for the asymmetry $n_l - n_{\bar{l}}$.

A typical solution of the Boltzmann equations (13) - (15) is shown in fig. 6. Here the ratios of number densities and entropy density,

$$Y_X = \frac{n_X}{s}, \quad (20)$$

are plotted, which remain constant in an expanding universe in thermal equilibrium. A heavy neutrino, which is weakly coupled to the thermal bath, falls out of thermal equilibrium at temperatures $T \sim M$ since its decay is too slow to follow the rapidly decreasing equilibrium distribution $f_N \sim \exp(-\beta M)$. This leads to an excess of the number density, $n_N > n_N^{eq}$. CP violating partial decay widths then yield a lepton asymmetry which, by means of sphaleron processes, is partially transformed into a baryon asymmetry.

The Boltzmann equations are classical equations for the time evolution of number densities. The collision terms, however, are S -matrix elements which involve quantum mechanical interferences of different amplitudes in a crucial manner. Since these scattering matrix elements are evaluated at zero temperature, one may worry to what extent the quantum mechanical interferences are affected by interactions with the thermal bath. A full quantum mechanical treatment can be based either on the density matrix [20] or on the Kadanoff-Baym equations [21].

Another subtlety is the separation of the $2 \rightarrow 2$ matrix elements into a resonance contribution and remainder [17],

$$|\mathcal{M}(l\phi \rightarrow \bar{l}\bar{\phi})|^2 = |\mathcal{M}'(l\phi \rightarrow \bar{l}\bar{\phi})|^2 + |\mathcal{M}_{res}(l\phi \rightarrow \bar{l}\bar{\phi})|^2, \quad (21)$$

where the resonance contribution has the form

$$\mathcal{M}_{res}(l\phi \rightarrow \bar{l}\bar{\phi}) \propto \mathcal{M}(l\phi \rightarrow N)\mathcal{M}(N \rightarrow \bar{l}\bar{\phi})^* = |\mathcal{M}(l\phi \rightarrow N)|^2. \quad (22)$$

The entire effect of baryon number generation crucially depends on this separation. The particles which participate in the $2 \rightarrow 2$ processes are massless, hence their distribution functions always coincide with the equilibrium distribution. Only the resonances, treated as on-shell particles, fall out of thermal equilibrium and can therefore generate an asymmetry in their decays. General theoretical arguments require cancellations between these two types of contributions which is illustrated by the following example.

2.2. CANCELLATIONS IN THERMAL EQUILIBRIUM

If all processes, including those which violate baryon number, are in thermal equilibrium the baryon asymmetry vanishes. This is a direct consequence of the CPT invariance of the theory,

$$\begin{aligned} \langle B \rangle &= \text{Tr}(\rho B) = \text{Tr}\left((CPT)(CPT)^{-1} \exp(-\beta H) B\right) \\ &= \text{Tr}\left(\exp(-\beta H)(CPT)^{-1} B(CPT)\right) = -\text{Tr}(\rho B) = 0. \end{aligned} \quad (23)$$

Hence, no asymmetry can be generated in equilibrium, and the transition rate which determines the change of the asymmetry has to vanish,

$$\frac{d(n_l - n_{\bar{l}})}{dt} + 3H(n_l - n_{\bar{l}}) \equiv \Delta\gamma^{eq} = 0, \quad (24)$$

where the superscript eq denotes rates evaluated with equilibrium distributions.

From eqs. (12), (14) and (15) one obtains for the resonance contribution, i.e. decay and inverse decay,

$$\Delta\gamma_{res}^{eq} = -2\epsilon\gamma^{eq}(N \rightarrow l\phi). \quad (25)$$

This means in particular that the asymmetry generated in the decay is not compensated by the effect of inverse decays. On the contrary, both processes contribute the same amount.

The rate $\Delta\gamma_{res}^{eq}$ has to be compensated by the contribution from $2 \rightarrow 2$ processes which is given by

$$\Delta\gamma_{2 \rightarrow 2}^{eq} = 2 \int d\Phi_{1234} f_l^{eq}(p_1) f_\phi^{eq}(p_2) \left(|\mathcal{M}'(l\phi \rightarrow \bar{l}\bar{\phi})|^2 - |\mathcal{M}'(\bar{l}\bar{\phi} \rightarrow l\phi)|^2 \right). \quad (26)$$

For weakly coupled heavy neutrinos, i.e. $\Gamma \propto \lambda^2 M$ with $\lambda^2 \ll 1$, this compensation can be easily shown using the unitarity of the S -matrix.

The sum over states in the unitarity relation,

$$\sum_X \left(|\mathcal{M}(l\phi \rightarrow X)|^2 - |\mathcal{M}(X \rightarrow l\phi)|^2 \right) = 0, \quad (27)$$

can be restricted to two-particle states to leading order in the case of weak coupling λ . This implies for the considered $2 \rightarrow 2$ processes,

$$\sum'_{l,\phi,\bar{l},\bar{\phi}'} \left(|\mathcal{M}(l\phi \rightarrow \bar{l}\bar{\phi}')|^2 - |\mathcal{M}(\bar{l}\bar{\phi}' \rightarrow l\phi)|^2 \right) = 0, \quad (28)$$

where the summation \sum' includes momentum integrations under the constraint of fixed total momentum. From eqs. (21) and (28) one obtains

$$\begin{aligned} \Delta\gamma_{2 \rightarrow 2}^{eq} &= 2 \int d\Phi_{1234} f_l^{eq}(p_1) f_\phi^{eq}(p_2) \\ &\quad \left(-|\mathcal{M}_{res}(l\phi \rightarrow \bar{l}\bar{\phi})|^2 + |\mathcal{M}_{res}(\bar{l}\bar{\phi} \rightarrow l\phi)|^2 \right). \end{aligned} \quad (29)$$

In the narrow width approximation, i.e. to leading order in λ^2 , this yields the wanted result,

$$\begin{aligned} \Delta\gamma_{2 \rightarrow 2}^{eq} &= 2 \int d\Phi_{1234} f_l^{eq}(p_1) f_\phi^{eq}(p_2) \left(-|\mathcal{M}(l\phi \rightarrow N)|^2 |\mathcal{M}(N \rightarrow \bar{l}\bar{\phi})|^2 \right. \\ &\quad \left. + |\mathcal{M}(\bar{l}\bar{\phi} \rightarrow N)|^2 |\mathcal{M}(N \rightarrow l\phi)|^2 \right) \frac{\pi}{M\Gamma} \delta(s - M^2) \\ &= 2\epsilon\gamma^{eq}(N \rightarrow l\phi) = -\Delta\gamma_{res}^{eq}. \end{aligned} \quad (30)$$

This cancellation also illustrates that the Boltzmann equations treat resonances as on-shell real particles. Off-shell effects can only be taken into account in a full quantum mechanical treatment.

3. Cosmological bounds on neutrino masses

Leptogenesis requires lepton number violation. On the other hand, the existence of a non-vanishing baryon asymmetry also restricts the allowed amount of lepton number violation and implies upper bounds on the Majorana masses of the light neutrinos.

In the standard model (SM) neutrinos are massless. In general, however, the exchange of heavy particles gives rise to an effective lepton Higgs interaction which, after electroweak symmetry breaking, generates neutrino masses. The lagrangian describing all fermion-Higgs couplings then reads

$$\begin{aligned} \mathcal{L}_Y = & -h_{dij}^T \overline{d_{Ri}} q_{Lj} H_1 - h_{uij}^T \overline{u_{Ri}} q_{Lj} H_2 - h_{eij} \overline{e_{Ri}} l_{Lj} H_1 \\ & + \frac{1}{2} f_{ij} l_{Li}^T H_2 C l_{Lj} H_2 + \text{h.c.} . \end{aligned} \quad (31)$$

Here q_{Li} , u_{Ri} , d_{Ri} , l_{Li} , e_{Ri} , $i = 1 \dots N$, are N generations of quark and lepton fields, H_1 and H_2 are Higgs fields with vacuum expectation values $v_i = \langle H_i^0 \rangle \neq 0$. h_d , h_u , h_e and f are $N \times N$ complex matrices. For the further discussion it is convenient to choose a basis where h_u and h_e are diagonal and real. In the case $v_1 \sim v_2 \sim v = \sqrt{v_1^2 + v_2^2}$ the smallest Yukawa coupling is $h_{e11} = m_e/v_1$ followed by $h_{u11} = m_u/v_2$.

The mixing of the different quark generations is given by the Kobayashi-Maskawa matrix V_d , which is defined by

$$h_d^T V_d = \frac{m_d}{v_1} . \quad (32)$$

Here m_d is the diagonal real down quark mass matrix, and the weak eigenstates of the right-handed d-quarks have been chosen to be identical to the mass eigenstates. Correspondingly, the mixing matrix V_ν in the leptonic charged current is determined by

$$V_\nu^T f V_\nu = - \frac{m_\nu}{v_2^2} , \quad (33)$$

where

$$m_\nu = \begin{pmatrix} m_1 & 0 & 0 \\ 0 & m_2 & 0 \\ 0 & 0 & m_3 \end{pmatrix} \quad (34)$$

is the diagonal and real mass matrix of the light Majorana neutrinos.

3.1. CHEMICAL EQUILIBRIUM

In a weakly coupled plasma with temperature T and volume V one can assign a chemical potential μ to each of the quark, lepton and Higgs fields. In the SM with one Higgs doublet, i.e., $H_2 = \tilde{H}_1 \equiv \varphi$, and N generations one has $5N+1$ chemical potentials. The corresponding partition function is [22]

$$Z(\mu, T, V) = \text{Tr} e^{-\beta(H - \sum_i \mu_i Q_i)}. \quad (35)$$

Here $\beta = 1/T$, H is the Hamilton operator and Q_i are the charge operators for the corresponding fields. The asymmetry in the particle and antiparticle number densities is then given by the derivative of the thermodynamic potential,

$$n_i - \bar{n}_i = -\frac{\partial \Omega(\mu, T)}{\partial \mu_i}, \quad \Omega(\mu, T) = -\frac{T}{V} \ln Z(\mu, T, V). \quad (36)$$

For a non-interacting gas of massless particles one has

$$n_i - \bar{n}_i = \frac{gT^3}{6} \begin{cases} \beta\mu_i + \mathcal{O}\left((\beta\mu_i)^3\right), & \text{fermions,} \\ 2\beta\mu_i + \mathcal{O}\left((\beta\mu_i)^3\right), & \text{bosons.} \end{cases} \quad (37)$$

The following analysis will be based on these relations for $\beta\mu_i \ll 1$. However, one should keep in mind that the plasma of the early universe is very different from a weakly coupled relativistic gas due to the presence of unscreened non-abelian gauge interactions. Hence, non-perturbative effects may be important in some cases.

In the high-temperature plasma quarks, leptons and Higgs bosons interact via Yukawa and gauge couplings and, in addition, via the non-perturbative sphaleron processes. In thermal equilibrium all these processes yield constraints between the various chemical potentials. The effective interaction (3) induced by the $SU(2)$ electroweak instantons yields the constraint [12],

$$\sum_i (3\mu_{qi} + \mu_{li}) = 0. \quad (38)$$

One also has to take the $SU(3)$ QCD instanton processes into account [23] which generate the effective interaction

$$O_A = \prod_i (q_{Li} q_{Li} u_{Ri}^c d_{Ri}^c) \quad (39)$$

between left-handed and right-handed quarks. The corresponding relation between the chemical potentials reads

$$\sum_i (2\mu_{qi} - \mu_{ui} - \mu_{di}) = 0. \quad (40)$$

A third condition, which is valid at all temperatures, arises from the requirement that the total hypercharge of the plasma vanishes. From eq. (37) and the known hypercharges one obtains

$$\sum_i \left(\mu_{qi} + 2\mu_{ui} - \mu_{di} - \mu_{li} - \mu_{ei} + \frac{2}{N}\mu_\varphi \right) = 0. \quad (41)$$

The Yukawa interactions, supplemented by gauge interactions, yield relations between the chemical potentials of left-handed and right-handed fermions,

$$\mu_{qi} - \mu_\varphi - \mu_{dj} = 0, \quad \mu_{qi} + \mu_\varphi - \mu_{uj} = 0, \quad \mu_{li} - \mu_\varphi - \mu_{ej} = 0. \quad (42)$$

Furthermore, the $\Delta L = 2$ interaction in (31) implies

$$\mu_{li} + \mu_\varphi = 0. \quad (43)$$

The above relations between chemical potentials hold if the corresponding interactions are in thermal equilibrium. In the temperature range $T_{EW} \sim 100 \text{ GeV} < T < T_{SPH} \sim 10^{12} \text{ GeV}$, which is of interest for baryogenesis, this is the case for all gauge interactions. It is not always true, however, for Yukawa interactions. The rate of a scattering process between left- and right-handed fermions, Higgs boson and W-boson,

$$\psi_L \varphi \rightarrow \psi_R W, \quad (44)$$

is $\Gamma \sim \alpha \lambda^2 T$, with $\alpha = g^2/(4\pi)$. This rate has to be compared with the Hubble rate,

$$H \simeq 0.33 g_*^{1/2} \frac{T^2}{M_{PL}} \simeq 0.1 g_*^{1/2} \frac{T^2}{10^{18} \text{ GeV}}. \quad (45)$$

The equilibrium condition $\Gamma(T) > H(T)$ is satisfied for sufficiently small temperatures,

$$T < T_\lambda \sim \lambda^2 10^{16} \text{ GeV}. \quad (46)$$

Hence, one obtains for the decoupling temperatures of right-handed electrons, up-quarks, ...,

$$T_e \sim 10^4 \text{ GeV}, \quad T_u \sim 10^6 \text{ GeV}, \dots \quad (47)$$

At a temperature $T \sim 10^{10} \text{ GeV}$, which is characteristic of leptogenesis, $e_R \equiv e_{R1}$, $\mu_R \equiv e_{R2}$, $d_R \equiv d_{R1}$, $s_R \equiv d_{R2}$ and $u_R \equiv u_{R1}$ are out of equilibrium.

Note that the QCD sphaleron constraint (40) is automatically satisfied if the quark Yukawa interactions are in equilibrium (cf. (42)). If the Yukawa

interaction of one of the right-handed quarks is too weak, the sphaleron constraint still establishes full chemical equilibrium.

Using eq. (37) also the baryon number density $n_B \equiv BT^2/6$ and the lepton number densities $n_L \equiv LT^2/6$ can be expressed in terms of the chemical potentials. The baryon asymmetry B and the lepton asymmetries L_i read

$$B = \sum_i (2\mu_{qi} + \mu_{ui} + \mu_{di}) , \quad (48)$$

$$L_i = 2\mu_{li} + \mu_{ei} , \quad L = \sum_i L_i . \quad (49)$$

3.2. RELATIONS BETWEEN B , L AND $B - L$

Knowing which particle species are in thermal equilibrium one can derive relations between different asymmetries. Consider first the most familiar case where all Yukawa interactions are in equilibrium and the $\Delta L = 2$ lepton-Higgs interaction is out of equilibrium. In this case the asymmetries $L_i - B/N$ are conserved. The Yukawa interactions establish equilibrium between the different generations,

$$\mu_{li} \equiv \mu_l , \quad \mu_{qi} \equiv \mu_q , \quad \text{etc.} \quad (50)$$

Together with the sphaleron process and the hypercharge constraint they allow to express all chemical potentials, and therefore all asymmetries, in terms of a single chemical potential which may be chosen to be μ_l . The result reads

$$\begin{aligned} \mu_e &= \frac{2N+3}{6N+3}\mu_l , & \mu_d &= -\frac{6N+1}{6N+3}\mu_l , & \mu_u &= \frac{2N-1}{6N+3}\mu_l , \\ \mu_q &= -\frac{1}{3}\mu_l , & \mu_\varphi &= \frac{4N}{6N+3}\mu_l . \end{aligned} \quad (51)$$

The corresponding baryon and lepton asymmetries are

$$B = -\frac{4N}{3}\mu_l , \quad L = \frac{14N^2+9N}{6N+3}\mu_l , \quad (52)$$

which yields the well-known connection between the B and $B - L$ asymmetries [24]

$$B = \frac{8N+4}{22N+13}(B-L) . \quad (53)$$

Note, that this relation only holds for temperatures $T \gg v$. In general, the ratio $B/(B-L)$ is a function of v/T [25, 26].

Another instructive example is the case where the $\Delta L = 2$ interactions are in equilibrium but the right-handed electrons are not. Depending on the neutrino masses and mixings, this could be the case for temperatures above $T_e \sim 10^4$ GeV [27]. Right-handed electron number would then be conserved, and Yukawa and gauge interactions would relate all asymmetries to the asymmetry of right-handed electrons. The various chemical potentials are given by ($\mu_e = \mu_{e1}, \mu_{\bar{e}} = \mu_{e2} = \dots = \mu_{eN}$),

$$\begin{aligned} \mu_{\bar{e}} &= -\frac{3}{10N}\mu_e, & \mu_d &= -\frac{1}{10N}\mu_e, & \mu_u &= \frac{1}{5N}\mu_e, \\ \mu_l &= -\frac{3}{20N}\mu_e, & \mu_q &= \frac{1}{20N}\mu_e, & \mu_\varphi &= \frac{3}{20N}\mu_e. \end{aligned} \quad (54)$$

The corresponding baryon and lepton asymmetries are [27]

$$B = \frac{1}{5}\mu_e, \quad L = \frac{4N+3}{10N}\mu_e, \quad (55)$$

which yields for the relation between B and $B - L$,

$$B = -\frac{2N}{2N+3}(B - L). \quad (56)$$

Note that although sphaleron processes and $\Delta L = 2$ processes are in equilibrium, the asymmetries in B , L and $B - L$ do not vanish!

3.3. CONSTRAINT ON MAJORANA NEUTRINO MASSES

The two examples illustrate the connection between lepton number and baryon number induced by sphaleron processes. They also show how this connection depends on other processes in the high-temperature plasma. To have one quark-Higgs or lepton-Higgs interaction out of equilibrium is sufficient in order to have non-vanishing B , L and $B - L$. If all interactions in (31) are in equilibrium, eqs. (43) and (51) together imply $\mu_l = 0$ and therefore

$$B = L = B - L = 0, \quad (57)$$

which is inconsistent with the existence of a matter-antimatter asymmetry. Since the equilibrium conditions of the various interactions are temperature dependent, and the $\Delta L = 2$ interaction is related to neutrino masses and mixings, one obtains important constraints on neutrino properties from the existence of the cosmological baryon asymmetry.

The $\Delta L = 2$ processes described by (9) take place with the rate [28]

$$\Gamma_{\Delta L=2}(T) = \frac{1}{\pi^3} \frac{T^3}{v^4} \sum_{i=e,\mu,\tau} m_{\nu_i}^2. \quad (58)$$

Requiring $\Gamma_{\Delta L=2}(T) < H(T)$ then yields an upper bound on Majorana neutrino masses,

$$\sum_i m_{\nu_i}^2 < \left(0.2 \text{ eV} \left(\frac{T_{SPH}}{T} \right)^{1/2} \right)^2. \quad (59)$$

For typical leptogenesis temperatures $T \sim 10^{10}$ GeV this bound is comparable to the upper bound on the electron neutrino mass obtained from neutrinoless double beta decay. Note, that the bound also applies to the τ -neutrino mass. However, if one uses for T the decoupling temperature of right-handed electrons, $T_e \sim 10^4$ GeV, the much weaker bound $m_\nu < 2$ keV is obtained [27].

Clearly, what temperature one has to use in eq. (59) depends on the thermal history of the early universe. Some information is needed on what kind of asymmetries may have been generated as the temperature decreased. This, together with the temperature dependence of the lepton-Higgs interactions then yields constraints on neutrino masses.

3.4. PRIMORDIAL ASYMMETRIES

The possible generation of asymmetries can be systematically studied by listing all the higher-dimensional $SU(3) \times SU(2) \times U(1)$ operators which may be generated by the exchange of heavy particles. The dynamics of the heavy particles may then generate an asymmetry in the quantum numbers carried by the massless fields which appear in the operator.

For $d=5$, there is a unique operator, which has already been discussed above,

$$(l_{Li}\varphi)(l_{Lj}\varphi). \quad (60)$$

It is generated in particular by the exchange of heavy Majorana neutrinos whose coupling to the massless fields is

$$h_{\nu ij} \overline{\nu_{Ri}} l_{Lj} \varphi. \quad (61)$$

The out-of-equilibrium decays of the heavy neutrinos can generate a lepton asymmetry, which is the well-known mechanism of leptogenesis. The decays yield asymmetries $L_i - B/N$ which are conserved in the subsequent evolution. The initial asymmetry in right-handed electrons is zero. In order to satisfy the out-of-equilibrium condition it is very important that at least some Yukawa couplings are small and that the right-handed neutrinos carry no quantum numbers with respect to unbroken gauge symmetries.

In order to study possible asymmetries of right-handed electrons one has to consider operators containing e_R . A simple example, with $d=6$, reads

$$(q_{Li} l_{Lj})(u_{Rk}^c e_{Rl}^c). \quad (62)$$

It can be generated by leptoquark exchange ($\chi \sim (3^*, 1, 1/3)$),

$$(\lambda_{ij}^q q_{Li}^T C l_{Lj} + \lambda_{ij}^u u_{Ri}^T C e_{Rj}) \chi. \quad (63)$$

Note, that $\tilde{\varphi}$ and χ form a 5^* -plet of $SU(5)$. In principle, out-of-equilibrium decays of leptoquarks may generate a e_R asymmetry. One may worry, however, whether the branching ratio into final states containing e_R is sufficiently large. Furthermore, it appears very difficult to satisfy the out-of-equilibrium condition since leptoquarks carry colour. Maybe, all these problems can be overcome by making use of coherent oscillations of scalar fields [8] or by special particle production mechanisms after inflation. However, we are not aware of a consistent scenario for the generation of a e_R -asymmetry. Hence, it appears appropriate to take the bound eq. (59) on Majorana neutrino masses as a guideline and to examine its validity in each particular model.

4. Neutrino masses and mixings

Majorana masses for the light neutrinos are most easily generated by the exchange of heavy Majorana neutrinos. Such heavy ‘right-handed’ neutrinos are predicted by all extensions of the standard model which contain $B - L$ as a local symmetry. The most general Lagrangian for couplings and masses of charged leptons and neutrinos reads

$$\mathcal{L}_Y = -h_{eij} \bar{e}_{Ri} l_{Lj} H_1 - h_{\nu ij} \bar{\nu}_{Ri} l_{Lj} H_2 - \frac{1}{2} h_{rij} \bar{\nu}_{Ri}^c \nu_{Rj} R + \text{h.c.} . \quad (64)$$

The vacuum expectation values of the Higgs fields, $\langle H_1 \rangle = v_1$ and $\langle H_2 \rangle = v_2 = \tan \beta v_1$, generate Dirac masses m_e and m_D for charged leptons and neutrinos, $m_e = h_e v_1$ and $m_D = h_\nu v_2$, respectively, which are assumed to be much smaller than the Majorana masses $M = h_r \langle R \rangle$. This yields light and heavy neutrino mass eigenstates according to the seesaw mechanism [29],

$$\nu \simeq V_\nu^T \nu_L + \nu_L^c V_\nu^* \quad , \quad N \simeq \nu_R + \nu_R^c, \quad (65)$$

with masses

$$m_\nu \simeq -V_\nu^T m_D^T \frac{1}{M} m_D V_\nu \quad , \quad m_N \simeq M. \quad (66)$$

Here V_ν is the mixing matrix in the leptonic charged current (cf. eqs. (31)-(33)).

In models of leptogenesis the predicted value of the baryon asymmetry depends on the CP asymmetry (cf. (12)) which is determined by the Dirac and the Majorana neutrino mass matrices. Depending on the neutrino mass hierarchy and the size of the mixing angles the CP asymmetry can vary over

many orders of magnitude. It is therefore important to see whether patterns of neutrino masses [30] motivated by other considerations are consistent with leptogenesis. In the following we shall consider two examples.

An attractive framework to explain the observed mass hierarchies of quarks and charged leptons is the Froggatt-Nielsen mechanism [31] based on a spontaneously broken $U(1)_F$ generation symmetry. The Yukawa couplings arise from non-renormalizable interactions after a gauge singlet field Φ acquires a vacuum expectation value,

$$h_{ij} = g_{ij} \left(\frac{\langle \Phi \rangle}{\Lambda} \right)^{Q_i + Q_j}. \quad (67)$$

Here g_{ij} are couplings $\mathcal{O}(1)$ and Q_i are the $U(1)_F$ charges of the various fermions, with $Q_\Phi = -1$. The interaction scale Λ is usually chosen to be very large, $\Lambda > \Lambda_{GUT}$. In the following we shall discuss two different realizations of this idea which are motivated by the atmospheric neutrino anomaly [32]. Both scenarios have a large $\nu_\mu - \nu_\tau$ mixing angle. They differ, however, by the symmetry structure and by the size of the parameter ϵ which characterizes the flavour mixing.

4.1. $SU(5) \times U(1)_F$

This symmetry has been considered by a number of authors. Particularly interesting is the case with a non-parallel family structure where the chiral $U(1)_F$ charges are different for the $\mathbf{5}^*$ -plets and the $\mathbf{10}$ -plets of the same family [33]-[37]. An example of possible charges Q_i is given in table 1.

The assignment of the same charge to the lepton doublets of the second and third generation leads to a neutrino mass matrix of the form [33, 34],

$$m_{\nu_{ij}} \sim \begin{pmatrix} \epsilon^2 & \epsilon & \epsilon \\ \epsilon & 1 & 1 \\ \epsilon & 1 & 1 \end{pmatrix} \frac{v_2^2}{\langle R \rangle}. \quad (68)$$

This structure immediately yields a large $\nu_\mu - \nu_\tau$ mixing angle. The phenomenology of neutrino oscillations depends on the unspecified coefficients

ψ_i	e_{R3}^c	e_{R2}^c	e_{R1}^c	l_{L3}	l_{L2}	l_{L1}	ν_{R3}^c	ν_{R2}^c	ν_{R1}^c
Q_i	0	1	2	0	0	1	0	1	2

TABLE 1. *Chiral charges of charged and neutral leptons with $SU(5) \times U(1)_F$ symmetry [37].*

$\mathcal{O}(1)$. The parameter ϵ which gives the flavour mixing is chosen to be

$$\frac{\langle \Phi \rangle}{\Lambda} = \epsilon \sim \frac{1}{17}, \quad (69)$$

which corresponds to the mass ratio m_μ/m_τ . The three Yukawa matrices for the leptons are given by,

$$h_e, h_\nu \sim \begin{pmatrix} \epsilon^3 & \epsilon^2 & \epsilon^2 \\ \epsilon^2 & \epsilon & \epsilon \\ \epsilon & 1 & 1 \end{pmatrix}, \quad h_r \sim \begin{pmatrix} \epsilon^4 & \epsilon^3 & \epsilon^2 \\ \epsilon^3 & \epsilon^2 & \epsilon \\ \epsilon^2 & \epsilon & 1 \end{pmatrix}. \quad (70)$$

Note, that h_e and h_ν have the same, non-symmetric structure. One easily verifies that the mass ratios for charged leptons, heavy and light Majorana neutrinos are given by

$$m_e : m_\mu : m_\tau \sim \epsilon^3 : \epsilon : 1, \quad M_1 : M_2 : M_3 \sim \epsilon^4 : \epsilon^2 : 1, \quad (71)$$

$$m_1 : m_2 : m_3 \sim \epsilon^2 : 1 : 1. \quad (72)$$

The masses of the two eigenstates ν_2 and ν_3 depend on the unspecified factors of order one, and may differ by an order of magnitude [38, 39]. They can therefore be consistent with the mass differences $\Delta m_{\nu_1\nu_2}^2 \simeq 4 \cdot 10^{-6} - 1 \cdot 10^{-5} \text{ eV}^2$ [40] inferred from the MSW solution of the solar neutrino problem [41] and $\Delta m_{\nu_2\nu_3}^2 \simeq (5 \cdot 10^{-4} - 6 \cdot 10^{-3}) \text{ eV}^2$ associated with the atmospheric neutrino deficit [32]. In the following we shall use for numerical estimates the average of the neutrino masses of the second and third family, $\overline{m}_\nu = (m_{\nu_2} m_{\nu_3})^{1/2} \sim 10^{-2} \text{ eV}$.

The choice of the charges in table 1 corresponds to large Yukawa couplings of the third generation. For the mass of the heaviest Majorana neutrino one finds

$$M_3 \sim \frac{v_2^2}{\overline{m}_\nu} \sim 10^{15} \text{ GeV}. \quad (73)$$

Since h_{r33} and the gauge coupling of $U(1)_{B-L}$ are $\mathcal{O}(1)$, this implies that $B-L$ is broken at the unification scale Λ_{GUT} .

4.2. $SU(3)_C \times SU(3)_L \times SU(3)_R \times U(1)_F$

This symmetry arises in unified theories based on the gauge group E_6 . The leptons e_R^c , l_L and ν_R^c are contained in a single $(1, 3, \overline{3})$ representation. Hence, all leptons of the same generation have the same $U(1)_F$ charge and all leptonic Yukawa matrices are symmetric. Masses and mixings of quarks and charged leptons can be successfully described by using the charges given

ψ_i	e_{R3}^c	e_{R2}^c	e_{R1}^c	l_{L3}	l_{L2}	l_{L1}	ν_{R3}^c	ν_{R2}^c	ν_{R1}^c
Q_i	0	$\frac{1}{2}$	$\frac{5}{2}$	0	$\frac{1}{2}$	$\frac{5}{2}$	0	$\frac{1}{2}$	$\frac{5}{2}$

TABLE 2. Chiral charges of charged and neutral leptons with $SU(3)_c \times SU(3)_L \times SU(3)_R \times U(1)_F$ symmetry [36].

in table 2. Clearly, all three Yukawa matrices have the same structure¹,

$$h_e, h_r \sim \begin{pmatrix} \epsilon^5 & \epsilon^3 & \epsilon^{5/2} \\ \epsilon^3 & \epsilon & \epsilon^{1/2} \\ \epsilon^{5/2} & \epsilon^{1/2} & 1 \end{pmatrix}, \quad h_\nu \sim \begin{pmatrix} \bar{\epsilon}^5 & \bar{\epsilon}^3 & \bar{\epsilon}^{5/2} \\ \bar{\epsilon}^3 & \bar{\epsilon} & \bar{\epsilon}^{1/2} \\ \bar{\epsilon}^{5/2} & \bar{\epsilon}^{1/2} & 1 \end{pmatrix}, \quad (74)$$

but the expansion parameter in h_ν may be different from the one in h_e and h_r . From the quark masses, which also contain ϵ and $\bar{\epsilon}$, one infers $\bar{\epsilon} \simeq \epsilon^2$ [36].

From eq. (74) one obtains for the masses of charged leptons, light and heavy Majorana neutrinos,

$$m_e : m_\mu : m_\tau \sim M_1 : M_2 : M_3 \sim \epsilon^5 : \epsilon : 1, \quad (75)$$

$$m_1 : m_2 : m_3 \sim \epsilon^{15} : \epsilon^3 : 1. \quad (76)$$

Like in the example with $SU(5) \times U(1)_F$ symmetry, the mass of the heaviest Majorana neutrino,

$$M_3 \sim \frac{v_2^2}{m_3} \sim 10^{15} \text{ GeV}, \quad (77)$$

implies that $B - L$ is broken at the unification scale Λ_{GUT} .

The $\nu_\mu - \nu_\tau$ mixing angle is related to the mixing of the charged leptons of the second and third generation [36],

$$\sin \Theta_{\mu\tau} \sim \sqrt{\bar{\epsilon}} + \epsilon. \quad (78)$$

This requires large flavour mixing,

$$\left(\frac{\langle \Phi \rangle}{\Lambda} \right)^{1/2} = \sqrt{\bar{\epsilon}} \sim \frac{1}{2}. \quad (79)$$

In view of the unknown coefficients $\mathcal{O}(1)$ the corresponding mixing angle $\sin \Theta_{\mu\tau} \sim 0.7$ is consistent with the interpretation of the atmospheric neutrino anomaly as $\nu_\mu - \nu_\tau$ oscillation.

¹Note, that with respect to ref. [36], ϵ and $\bar{\epsilon}$ have been interchanged.

It is very instructive to compare the two scenarios of lepton masses and mixings described above. In the first case, the large $\nu_\mu - \nu_\tau$ mixing angle follows from a non-parallel flavour symmetry. The parameter ϵ , which characterizes the flavour mixing, is small. In the second case, the large $\nu_\mu - \nu_\tau$ mixing angle is a consequence of the large flavour mixing ϵ . The $U(1)_F$ charges of all leptons are the same, i.e., one has a parallel family structure. Also the mass hierarchies, given in terms of ϵ , are rather different. This illustrates that the separation into a flavour mixing parameter ϵ and coefficients $\mathcal{O}(1)$ is far from unique. It is therefore important to study other observables which depend on the lepton mass matrices. This includes lepton flavour changing processes and, in particular, the cosmological baryon asymmetry.

5. Calculating the baryon asymmetry

5.1. MAJORANA NEUTRINO DECAYS

The heavy Majorana neutrinos, whose exchange may erase any lepton asymmetry, can also generate a lepton asymmetry by means of out-of-equilibrium decays. This lepton asymmetry is then partially transformed into a baryon asymmetry by sphaleron processes. The decay width of the heavy neutrino N_i reads at tree level,

$$\Gamma_{Di} = \Gamma(N_i \rightarrow H_2 + l) + \Gamma(N_i \rightarrow H_2^c + l^c) = \frac{1}{8\pi} (h_\nu h_\nu^\dagger)_{ii} M_i. \quad (80)$$

A necessary requirement for baryogenesis is the out-of-equilibrium condition $\Gamma_{D1} < H|_{T=M_1}$ [42], where H is the Hubble parameter at temperature T . From the decay width (80) one then obtains an upper bound on an effective light neutrino mass [43, 44],

$$\begin{aligned} \tilde{m}_1 &= (h_\nu h_\nu^\dagger)_{11} \frac{v_2^2}{M_1} \simeq 4g_*^{1/2} \frac{v_2^2}{M_P} \frac{\Gamma_{D1}}{H} \Big|_{T=M_1} \\ &< 10^{-3} \text{ eV}. \end{aligned} \quad (81)$$

Here g_* is the number of relativistic degrees of freedom, $M_P = (8\pi G_N)^{-1/2} \simeq 2.4 \cdot 10^{18}$ GeV is the Planck mass, and we have assumed $g_* \simeq 100$, $v_2 \simeq 174$ GeV. More direct bounds on the light neutrino masses depend on the structure of the Dirac neutrino mass matrix. If the bound (81) is satisfied, the heavy neutrinos N_1 are not able to follow the rapid change of the equilibrium distribution once the temperature of the universe drops below the mass M_1 . Hence, the deviation from thermal equilibrium consists in a too large number density of heavy neutrinos N_1 as compared to the equilibrium density (cf. section 2.1).

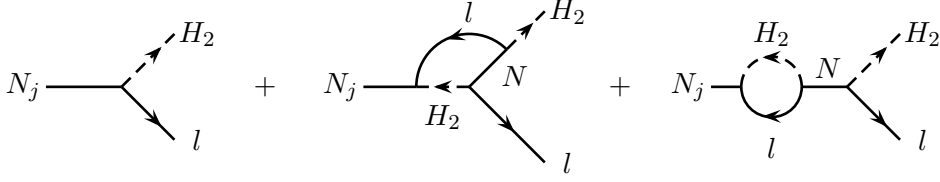


Figure 7. Tree level and one-loop diagrams contributing to heavy neutrino decays.

Eventually, however, the neutrinos will decay, and a lepton asymmetry is generated due to the CP asymmetry which comes about through interference between the tree-level amplitude and the one-loop diagrams shown in fig. 7. In a basis, where the right-handed neutrino mass matrix $M = h_r \langle R \rangle$ is diagonal, one obtains

$$\begin{aligned} \varepsilon_1 &= \frac{\Gamma(N_1 \rightarrow l H_2) - \Gamma(N_1 \rightarrow l^c H_2^c)}{\Gamma(N_1 \rightarrow l H_2) + \Gamma(N_1 \rightarrow l^c H_2^c)} \\ &\simeq \frac{1}{8\pi} \frac{1}{(h_\nu h_\nu^\dagger)_{11}} \sum_{i=2,3} \text{Im} \left[(h_\nu h_\nu^\dagger)_{1i}^2 \right] \left[f \left(\frac{M_i^2}{M_1^2} \right) + g \left(\frac{M_i^2}{M_1^2} \right) \right]; \end{aligned} \quad (82)$$

here f is the contribution from the one-loop vertex correction,

$$f(x) = \sqrt{x} \left[1 - (1+x) \ln \left(\frac{1+x}{x} \right) \right], \quad (83)$$

and g denotes the contribution from the one-loop self energy [45, 46, 47], which can be reliably calculated in perturbation theory for sufficiently large mass splittings, i.e., $|M_i - M_1| \gg |\Gamma_i - \Gamma_1|$,

$$g(x) = \frac{\sqrt{x}}{1-x}. \quad (84)$$

For $M_1 \ll M_2, M_3$ one obtains

$$\varepsilon_1 \simeq -\frac{3}{16\pi} \frac{1}{(h_\nu h_\nu^\dagger)_{11}} \sum_{i=2,3} \text{Im} \left[(h_\nu h_\nu^\dagger)_{1i}^2 \right] \frac{M_1}{M_i}. \quad (85)$$

In the case of mass differences of order the decay widths one expects an enhancement from the self-energy contribution [48].

The CP asymmetry (82) leads to a lepton asymmetry [42],

$$Y_L = \frac{n_L - n_{\bar{L}}}{s} = \kappa \frac{\varepsilon_1}{g_*}. \quad (86)$$

Here the factor $\kappa < 1$ represents the effect of washout processes. In order to determine κ one has to solve the full Boltzmann equations [18, 19]. In the examples discussed in sections 4.1 and 4.2 one obtains $\kappa \simeq 10^{-1} \dots 10^{-3}$. Important processes are the $\Delta L = 2$ lepton Higgs scatterings mediated by heavy neutrinos (cf. fig. 5) since cancellations between on-shell contributions to these scatterings and contributions from neutrino decays and inverse decays ensure that no asymmetry is generated in thermal equilibrium [17]. Further, due to the large top-quark Yukawa coupling one has to take into account neutrino top-quark scatterings mediated by Higgs bosons [18, 19]. These processes are of crucial importance for leptogenesis, since they can create a thermal population of heavy neutrinos at high temperatures $T > M_1$. Alternatively, the density of heavy neutrinos may be generated by inflaton decays [49]. Obviously, the requested baryon asymmetry can only be generated if the heavy neutrinos are sufficiently numerous before decaying.

Leptogenesis has been considered for various extensions of the standard model (cf. [16]). In particular, it is intriguing that in the simple case of hierarchical heavy neutrino masses the observed value of the baryon asymmetry is obtained without any fine tuning of parameters if $B - L$ is broken at the unification scale, $\Lambda_{GUT} \sim 10^{16}$ GeV [50]. The corresponding light neutrino masses are very small, i.e., $m_{\nu_2} \sim 3 \cdot 10^{-3}$ eV, as preferred by the MSW explanation of the solar neutrino deficit, and $m_{\nu_3} \sim 0.1$ eV. Such small neutrino masses are also consistent with the atmospheric neutrino anomaly [32], which implies a small mass m_{ν_3} in the case of hierarchical neutrino masses. This fact gave rise to a renewed interest in leptogenesis in recent years.

5.2. BARYON ASYMMETRY AND BARYOGENESIS TEMPERATURE

We can now evaluate the baryon asymmetry for the two patterns of neutrino mass matrices discussed in sections 4.1 and 4.2. Since for the Yukawa couplings only the powers in ϵ are known, we will also obtain the CP asymmetries and the corresponding baryon asymmetries to leading order in ϵ , i.e., up to unknown factors $\mathcal{O}(1)$. Note, that for models with a $U(1)_F$ generation symmetry the baryon asymmetry is ‘quantized’, i.e., changing the $U(1)_F$ charges will change the baryon asymmetry by powers of ϵ [37].

5.2.1. $SU(5) \times U(1)_F$

In this case one obtains from eqs. (82) and (70),

$$\varepsilon_1 \sim \frac{3}{16\pi} \epsilon^4. \quad (87)$$

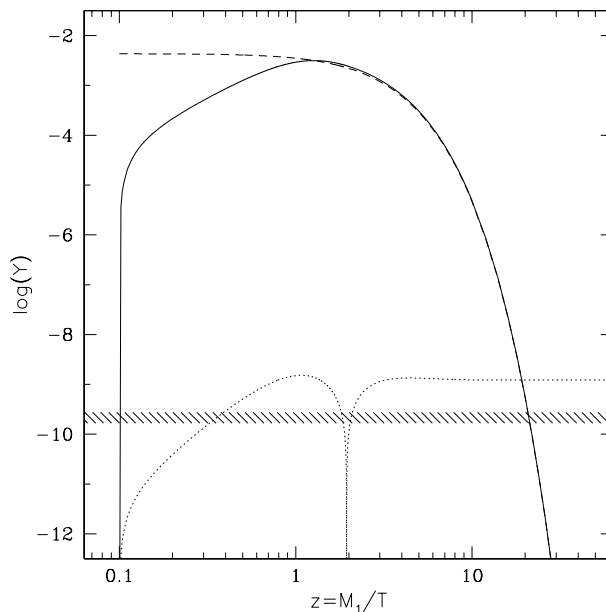


Figure 8. Time evolution of the neutrino number density and the lepton asymmetry for the $SU(5) \times U(1)_F$ model. The solid line shows the solution of the Boltzmann equation for the right-handed neutrinos, while the corresponding equilibrium distribution is represented by the dashed line. The absolute value of the lepton asymmetry Y_L is given by the dotted line and the hatched area shows the lepton asymmetry corresponding to the observed baryon asymmetry.

From eq. (86), $\epsilon^2 \sim 1/300$ (69) and $g_* \sim 100$ one then obtains the baryon asymmetry,

$$Y_B \sim \kappa 10^{-8} . \quad (88)$$

For $\kappa \sim 0.1 \dots 0.01$ this is indeed the correct order of magnitude! The baryogenesis temperature is given by the mass of the lightest of the heavy Majorana neutrinos,

$$T_B \sim M_1 \sim \epsilon^4 M_3 \sim 10^{10} \text{ GeV} . \quad (89)$$

For this model, where the CP asymmetry is determined by the mass hierarchy of light and heavy Majorana neutrinos, baryogenesis has been studied in detail in [50]. The generated baryon asymmetry does not depend on the flavour mixing of the light neutrinos, in particular the $\nu_\mu - \nu_\tau$ mixing angle.

The solution of the full Boltzmann equations is shown in fig. 8 for the non-supersymmetric case; the supersymmetric model has been studied in [51]. The initial condition at a temperature $T \sim 10M_1$ is chosen to be a state without heavy neutrinos. The Yukawa interactions are sufficient to bring

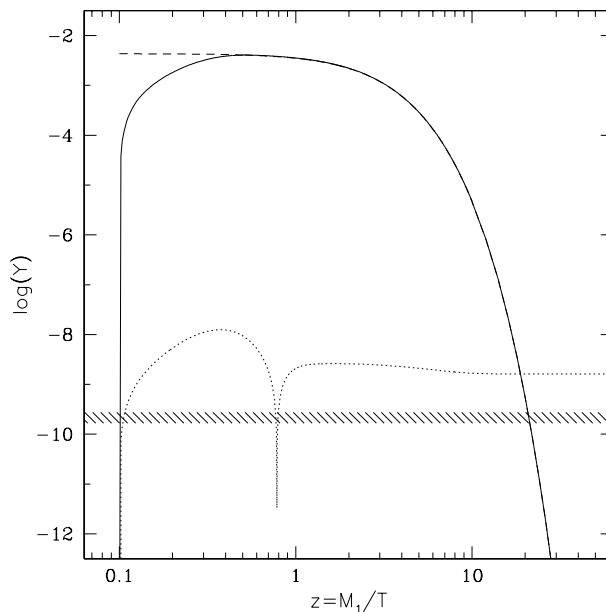


Figure 9. Solution of the Boltzmann equations for the $SU(3)_c \times SU(3)_L \times SU(3)_R \times U(1)_F$ model.

the heavy neutrinos into thermal equilibrium. The approach of the heavy neutrino number density to the equilibrium density and the evolution of the lepton asymmetry are analogous to GUT baryogenesis with heavy bosons [52]. At temperatures $T \sim M_1$ the familiar out-of-equilibrium decays sets in, which leads to a non-vanishing baryon asymmetry. The final asymmetry agrees with the estimate (88) for $\kappa \sim 0.1$. The dip in fig. 8 is due to a change of sign in the lepton asymmetry at $T \sim M_1$.

5.2.2. $SU(3)_c \times SU(3)_L \times SU(3)_R \times U(1)_F$

In this model the neutrino Yukawa couplings (74) yield the CP asymmetry

$$\varepsilon_1 \sim \frac{3}{16\pi} \epsilon^5, \quad (90)$$

which correspond to the baryon asymmetry (cf. (86))

$$Y_B \sim \kappa 10^{-6}. \quad (91)$$

Due to the large value of ϵ the CP asymmetry is two orders of magnitude larger than in the $SU(5) \times U(1)_F$ model. However, washout processes are now also stronger. The solution of the Boltzmann equations is shown in fig. 9. The final asymmetry is again $Y_B \sim 10^{-9}$ which corresponds to $\kappa \sim$

10^{-3} . The baryogenesis temperature is considerably larger than in the first case,

$$T_B \sim M_1 \sim \epsilon^5 M_3 \sim 10^{12} \text{ GeV} . \quad (92)$$

The baryon asymmetry is largely determined by the parameter \tilde{m}_1 defined in eq. (81) [19]. In the first example, one has $\tilde{m}_1 \sim \bar{m}_\nu$. In the second case one finds $\tilde{m}_1 \sim m_3$. Since \bar{m}_ν and m_3 are rather similar it is not too surprising that the generated baryon asymmetry is about the same in both cases.

6. Implications for dark matter

The experimental evidence for small neutrino masses, the see-saw mechanism and the out-of-equilibrium condition for the decay of the heavy Majorana neutrinos are all consistent and suggest rather large heavy neutrino masses and a correspondingly large baryogenesis temperature. For thermal leptogenesis models one typically finds [16],

$$T_B \sim M_1 > 10^7 \text{ GeV} . \quad (93)$$

In the particularly attractive supersymmetric version of thermal leptogenesis one then has to consider the following two issues: the consistency of the large baryogenesis temperature with the ‘gravitino constraint’ and the size of other possible contributions to the baryon asymmetry. A large asymmetry can in principle be generated by coherent oscillations of scalar fields which carry baryon and lepton number [8]. It appears likely, however, that the interactions of the right-handed neutrinos are sufficiently strong to erase such primordial baryon and lepton asymmetries before thermal leptogenesis takes place [53].

The couplings of gravitinos with matter are essentially model independent. Their cosmological effects therefore provide very interesting information about possible extensions of the standard model. It was realized long

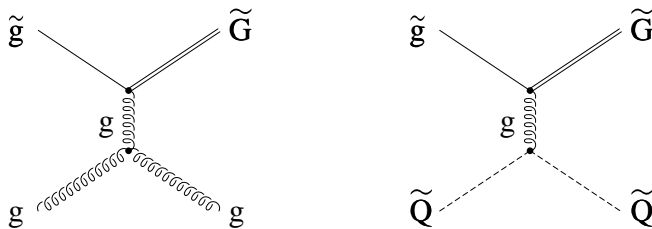


Figure 10. Typical gravitino production processes mediated by gluon exchange.

ago that standard cosmology requires gravitinos to be either very light, $m_{\tilde{G}} < 1 \text{ keV}$ [54], or very heavy, $m_{\tilde{G}} > 10 \text{ TeV}$ [55]. These constraints are relaxed if the standard cosmology is extended to include an inflationary phase [56, 57, 58]. The cosmologically relevant gravitino abundance is then created in the reheating phase after inflation in which a reheating temperature T_R is reached. Gravitinos are dominantly produced by inelastic $2 \rightarrow 2$ scattering processes of particles from the thermal bath. The gravitino abundance is essentially linear in the reheating temperature T_R . It is intriguing that for temperatures $T_R \sim 10^{10} \text{ GeV}$, which are of interest for leptogenesis, gravitinos with mass of the electroweak scale, $m_{\tilde{G}} \sim 100 \text{ GeV}$, can be the dominant component of cold dark matter [59].

The bounds on the reheating temperature depend on the thermal gravitino production rate which is dominated by two-body processes involving gluinos (\tilde{g}) (cf. fig. 10). On dimensional grounds the production rate has the form

$$\Gamma(T) \propto \frac{1}{M^2} T^3, \quad (94)$$

where $M = (8\pi G_N)^{-1/2} = 2.4 \cdot 10^{18} \text{ GeV}$ is the Planck mass. Hence, the density of thermally produced gravitinos increases strongly with temperature.

The production rate depends on the ratio $m_{\tilde{g}}/m_{\tilde{G}}$, the ratio of gluino and gravitino masses. The ten $2 \rightarrow 2$ gravitino production processes were considered in [57] for $m_{\tilde{g}} \ll m_{\tilde{G}}$. The case $m_{\tilde{g}} \gg m_{\tilde{G}}$, where the goldstino contribution dominates, was studied in [58]. Four of the ten production processes are logarithmically singular due to the exchange of massless gluons. The complete result for the logarithmically singular part of the production rate was obtained in [59]. The correct finite part can be obtained by means of a hard thermal loop resummation, which was first implemented in the case of axion production in a QED plasma [60] and recently also for gravitino production in a QCD plasma [61]. The result for the Boltzmann collision term reads

$$C_{\tilde{G}}(T) = \left(1 + \frac{m_{\tilde{g}}^2}{3m_{\tilde{G}}^2}\right) \frac{3\zeta(3)g^2(N^2 - 1)T^6}{32\pi^3 M^2} \times \left\{ \left[\ln\left(\frac{T^2}{m_{\tilde{g}}^2}\right) + 0.3224 \right] (N + n_f) + 0.5781n_f \right\}, \quad (95)$$

where

$$m_g^2 = \frac{g^2 T^2}{6} (N + n_f) \quad (96)$$

is the thermal gluon mass squared; N is the number of colours and n_f is the number of colour triplet and anti-triplet chiral multiplets. The QCD

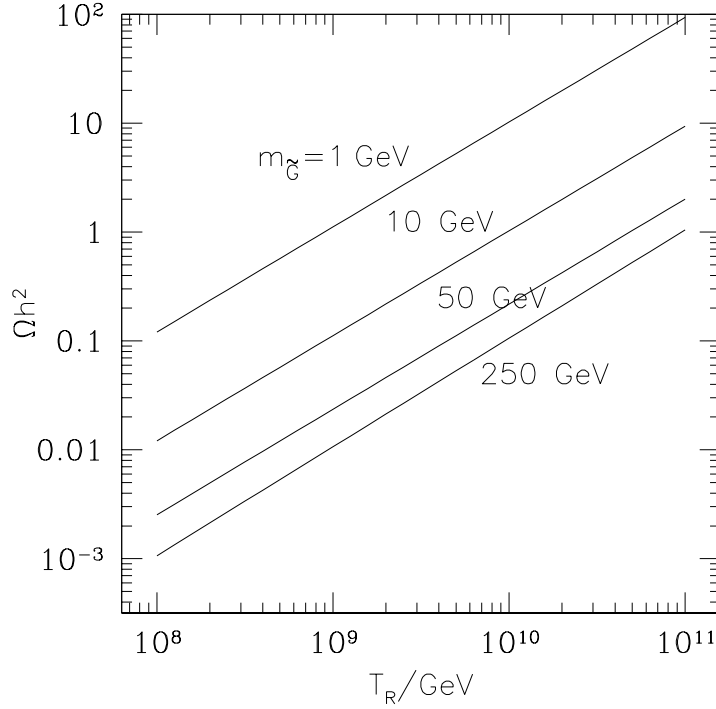


Figure 11. Contribution of gravitinos to the density parameter $\Omega_{\tilde{G}} h^2$ for different gravitino masses $m_{\tilde{G}}$ as function of the reheating temperature T_R . The gluino mass has been set to $m_{\tilde{g}} = 700$ GeV [61].

coupling $g(T) \simeq 0.85$ for $T \sim 10^{10}$ GeV. For the supersymmetric standard model with $N_C = 3$ and $n_f = 6$ this implies $m_g > T$. Hence, the usually assumed separation of scales, $g^2 T \ll gT \ll T$, appears problematic and higher-order corrections may be important.

Using the Boltzmann equation,

$$\frac{dn_{\tilde{G}}}{dt} + 3Hn_{\tilde{G}} = C_{\tilde{G}}, \quad (97)$$

one can calculate the gravitino abundance at temperatures $T < T_R$, assuming constant entropy. One finds

$$Y_{\tilde{G}}(T) = \frac{n_{\tilde{G}}(T)}{n_{\text{rad}}(T)} \simeq \frac{g_{*S}(T)}{g_{*S}(T_R)} \frac{C_{\tilde{G}}(T_R)}{H(T_R)n_{\text{rad}}(T_R)}, \quad (98)$$

where $g_{*S}(T)$ is the number of effectively massless degrees of freedom [2]. For $T < 1$ MeV, i.e. after nucleosynthesis, $g_{*S}(T) = \frac{43}{11}$, whereas

$g_{*S}(T_R) = \frac{915}{4}$ in the supersymmetric standard model. With $H(T) = (g_*(T)\pi^2/90)^{1/2}T^2/M$ one obtains in the case of light gravitinos ($m_{\tilde{G}} \ll m_{\tilde{g}}(\mu)$, $\mu \simeq 100$ GeV) from eqs. (98) and (95) for the gravitino abundance and for the contribution to Ωh^2 ,

$$Y_{\tilde{G}} = 1.1 \cdot 10^{-10} \left(\frac{T_R}{10^{10} \text{ GeV}} \right) \left(\frac{100 \text{ GeV}}{m_{\tilde{G}}} \right)^2 \left(\frac{m_{\tilde{g}}(\mu)}{1 \text{ TeV}} \right)^2, \quad (99)$$

$$\begin{aligned} \Omega_{\tilde{G}} h^2 &= m_{\tilde{G}} Y_{\tilde{G}}(T) n_{\text{rad}}(T) h^2 \rho_c^{-1} \\ &= 0.21 \left(\frac{T_R}{10^{10} \text{ GeV}} \right) \left(\frac{100 \text{ GeV}}{m_{\tilde{G}}} \right) \left(\frac{m_{\tilde{g}}(\mu)}{1 \text{ TeV}} \right)^2. \end{aligned} \quad (100)$$

Here we have used $n_{\text{rad}}(T) = \zeta(3)T^3/\pi^2$, and $m_{\tilde{g}}(T) = g^2(T)/g^2(\mu)m_{\tilde{g}}(\mu)$. The new result for $\Omega_{\tilde{G}} h^2$ is smaller by a factor of 3 compared to the result given in [59]. This is due to a partial cancellation between the logarithmic term and the constant term in eq. (95).

It is remarkable that reheating temperatures $T_R = 10^8 - 10^{10}$ GeV lead to values $\Omega_{\tilde{G}} h^2 = 0.01 \dots 1$ in an interesting gravitino mass range. This is illustrated in fig. 11 for a gluino mass $m_{\tilde{g}} = 700$ GeV. As an example, for $T_R \simeq 10^{10}$ GeV, $m_{\tilde{G}} \simeq 80$ GeV and $h \simeq 0.65$ [2] one finds $\Omega_{\tilde{G}} = 0.35$, which agrees with recent measurements of the matter density Ω_M [2].

In general, to find a viable cosmological scenario one has to avoid two types of gravitino problems: For unstable gravitinos their decay products must not alter the observed abundances of light elements in the universe, which is referred to as the big bang nucleosynthesis (BBN) constraint. For stable gravitinos this condition has to be met by other super particles, in particular the next-to-lightest super particle (NSP), which decays into gravitinos; further, their contribution to the energy density of the universe must not exceed the closure limit, i.e. $\Omega_{\tilde{G}} = \rho_{\tilde{G}}/\rho_c < 1$, where $\rho_c = 3H_0^2 M^2 = 1.05 h^2 10^{-5} \text{ GeV cm}^{-3}$ is the critical energy density.

Consider first the constraint from the closure limit. The condition $\Omega_{\tilde{G}} = Y_{\tilde{G}} m_{\tilde{G}} n_{\text{rad}}/\rho_c \leq 1$ yields a boundary in the $m_{\tilde{G}}-m_{\tilde{g}}$ plane which is shown in fig. 12 for three different values of the reheating temperature T_R . The allowed regions are below the three solid lines, respectively.

With respect to the BBN constraint, consider some nonrelativistic particle X which decays into electromagnetically and strongly interacting relativistic particles with a lifetime τ_X . Roughly speaking, the decay changes the abundances of light elements the more the longer the lifetime τ_X and the higher the energy density $m_X Y_X$ are. These constraints have been studied in detail by several groups [62, 63, 64]. For most supergravity models they rule out the possibility of unstable gravitinos with $m_{\tilde{G}} \sim 100$ GeV for

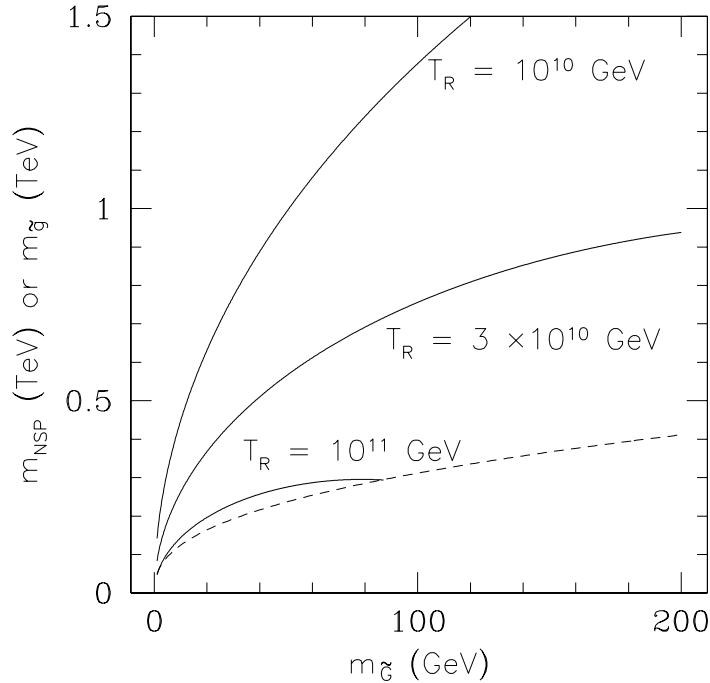


Figure 12. Upper and lower bounds on the gluino mass and the NSP mass as functions of the gravitino mass. The full lines represent the upper bound on the gluino mass $m_{\tilde{g}} > m_{NSP}$ for different reheating temperatures from the closure limit constraint. The dashed line is the lower bound on m_{NSP} which follows from the NSP lifetime [61].

$T_R \sim 10^{10}$ GeV, although even larger reheating temperatures are acceptable in some cases [65].

For stable gravitinos the NSP plays the role of the particle X. The lifetime of a fermion decaying into its scalar partner and a gravitino is

$$\tau_{NSP} = 48\pi \frac{m_{\tilde{G}}^2 M^2}{m_{NSP}^5}. \quad (101)$$

For a sufficiently short lifetime, $\tau_{NSP} < 2 \cdot 10^6$ s, it is sufficient to require the energy density which becomes free in NSP decays to be smaller than $m_X Y_X < 4 \cdot 10^{-10}$ GeV, which corresponds to $\Omega_X h^2 < 0.008$. This constraint can be satisfied since the NSP relic density is rather model dependent. For neutralinos in the MSSM the energy fraction Ω_χ can vary over eight orders of magnitude (cf. fig. (13)). The lifetime constraint $\tau_{NSP} <$

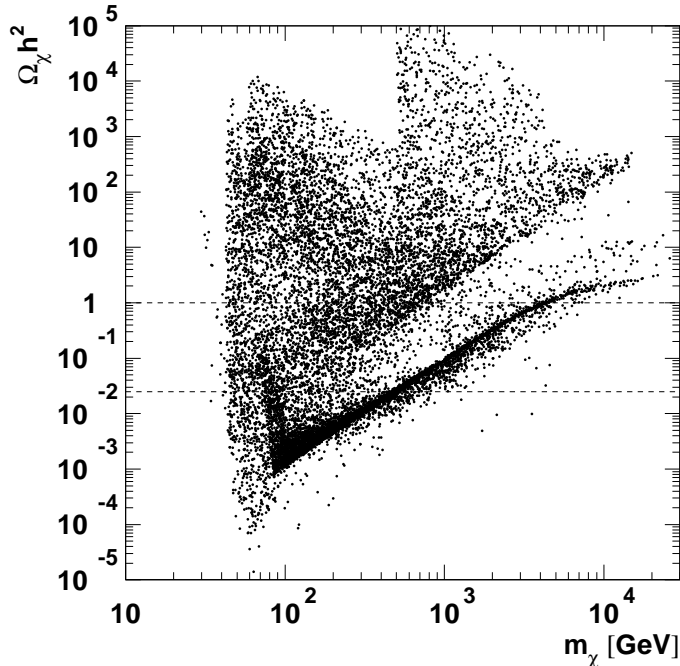


Figure 13. Neutralino relic density versus neutralino mass. The horizontal lines bound the region $0.025 < \Omega_\chi h^2 < 1$ [70].

$2 \cdot 10^6$ s yields a lower bound on super particle masses which is represented by the dashed line in the $m_{\tilde{G}}-m_{\text{NSP}/\tilde{g}}$ plane in fig. 12.

In order to decide whether the second part of the BBN constraint, $\Omega_{\text{NSP}} h^2 < 0.008$, is satisfied, one has to specify which particle is the NSP. The case of a higgsino-like neutralino as NSP has been studied in [59]. A detailed discussion for a scalar τ -lepton as NSP has been given in [66],[67].

7. Outlook

Recent developments in theoretical and experimental particle physics support the idea of leptogenesis according to which the cosmological matter density has been created in decays of heavy Majorana neutrinos. On the theoretical side, detailed studies of the electroweak phase transition and sphaleron processes have shown that the matter-antimatter asymmetry is related to neutrino properties. On the experimental side, the solar and atmospheric neutrino deficits have been observed, which can be interpreted

as a result of oscillations between three species of light Majorana neutrinos.

It is very remarkable that these hints on the nature of lepton number violation fit very well together with the leptogenesis mechanism. For hierarchical neutrino masses, with $B - L$ broken at the unification scale $\Lambda_{\text{GUT}} \sim 10^{16}$ GeV, the observed baryon asymmetry $n_B/s \sim 10^{-10}$ is naturally explained by the decay of heavy Majorana neutrinos. The corresponding baryogenesis temperature is $T_B \sim 10^{10}$ GeV.

The consistency of this picture has implications in particle physics and cosmology. In unified theories the pattern of neutrino masses and mixings is related to lepton flavour and quark flavour changing processes. In supersymmetric theories the mass spectrum of superparticles is constrained by the cosmological bound on the number density of gravitinos which may be the dominant component of dark matter. Further, the realization of the rather large baryogenesis temperature in models of inflation should have observable consequences for the anisotropy of the cosmic microwave background.

Acknowledgements

The content of these lectures is based on work in collaboration with M. Bolz, A. Brandenburg, S. Fredenhagen, M. Plümacher and T. Yanagida whom I thank for a fruitful collaboration. I am also grateful to the organizers for arranging an enjoyable and stimulating meeting.

References

1. P. de Bernardis et al., *Nature* **404** (2000) 955
2. Review of Particle Physics, *Eur. Phys. J.* **C15** (2000) 1
3. R. Fleischer, these proceedings
4. A. D. Sakharov, *JETP Lett.* **5** (1967) 24
5. G. 't Hooft, *Phys. Rev. Lett.* **37** (1976) 8; *Phys. Rev.* **D 14** (1976) 3422
6. M. Yoshimura, *Phys. Rev. Lett.* **41** (1978) 281; *ibid.* **42** (1979) 746 (E);
S. Dimopoulos, L. Susskind, *Phys. Rev.* **D 18** (1978) 4500;
D. Toussaint, S. B. Treiman, F. Wilczek, A. Zee, *Phys. Rev.* **D 19** (1979) 1036;
S. Weinberg, *Phys. Rev. Lett.* **42** (1979) 850
7. M. Fukugita, T. Yanagida, *Phys. Lett.* **B 174** (1986) 45
8. I. Affleck, M. Dine, *Nucl. Phys.* **B 249** (1985) 361
9. C. Wetterich, these proceedings
10. A. Linde, these proceedings
11. For a review and references, see
A. Riotto, M. Trodden, *Ann. Rev. Nucl. Part. Sci.* **49** (1999) 35
12. V. A. Kuzmin, V. A. Rubakov, M. E. Shaposhnikov, *Phys. Lett.* **B 155** (1985) 36
13. D. Bödeker, *Phys. Lett.* **B 426** (1998) 351
14. G. D. Moore, *Do We Understand the Sphaleron Rate?*, [hep-ph/0009161](#)
15. J. A. Harvey, M. S. Turner, *Phys. Rev.* **D 42** (1990) 3344
16. For a review and references, see
W. Buchmüller, M. Plümacher, *Neutrino Masses and the Baryon Asymmetry*,
[hep-ph/0007176](#)
17. E. W. Kolb, S. Wolfram, *Nucl. Phys.* **B 172** (1980) 224; *Nucl. Phys.* **B 195** (1982)
542(E)
18. M. A. Luty, *Phys. Rev.* **D 45** (1992) 455
19. M. Plümacher, *Z. Phys.* **C 74** (1997) 549;
20. I. Joichi, S. Matsumoto, M. Yoshimura, *Phys. Rev.* **D 58** (1998) 43507
21. W. Buchmüller, S. Fredenhagen, *Phys. Lett.* **B 483** (2000) 217
22. L. D. Landau, E. M. Lifshitz, *Statistical Physics*, Addison-Wesley (1959)
23. R. N. Mohapatra, X. Zhang, *Phys. Rev.* **D 45** (1992) 2699
24. S. Yu. Khlebnikov, M. E. Shaposhnikov, *Nucl. Phys.* **B 308** (1988) 885
25. S. Yu. Khlebnikov, M. E. Shaposhnikov, *Phys. Lett.* **B 387** (1996) 817
26. M. Laine, M. E. Shaposhnikov, *Phys. Rev.* **D 61** (2000) 117302
27. J. M. Cline, K. Kainulainen, K. A. Olive, *Phys. Rev. Lett.* **71** (1993) 2372;
Phys. Rev. **D 49** (1994) 6394
28. M. Fukugita, T. Yanagida, *Phys. Rev.* **D 42** (1990) 1285
29. T. Yanagida, in *Workshop on unified Theories*, KEK report 79-18 (1979) p. 95;
M. Gell-Mann, P. Ramond, R. Slansky, in *Supergravity* (North Holland, Amsterdam,
1979) eds. P. van Nieuwenhuizen, D. Freedman, p. 315
30. E. Akhmedov, these proceedings
31. C. D. Froggatt, H. B. Nielsen, *Nucl. Phys.* **B 147** (1979) 277
32. Super-Kamiokande Collaboration, Y. Fukuda et al., *Phys. Rev. Lett.* **81** (1998) 1562
33. T. Yanagida, J. Sato, *Nucl. Phys. B Proc. Suppl.* **77** (1999) 293
34. P. Ramond, *Nucl. Phys. B Proc. Suppl.* **77** (1999) 3
35. J. Bijnens, C. Wetterich, *Nucl. Phys.* **B 292** (1987) 443
36. S. Lola, G. G. Ross, *Nucl. Phys.* **B 553** (1999) 81
37. W. Buchmüller, T. Yanagida, *Phys. Lett.* **B 445** (1999) 399
38. N. Irges, S. Lavignac, P. Ramond, *Phys. Rev.* **D 58** (1998) 035003
39. F. Vissani, *JHEP11* (1998) 025
40. N. Hata, P. Langacker, *Phys. Rev.* **D 56** (1997) 6107
41. S. P. Mikheyev, A. Y. Smirnov, *Nuovo Cim.* **9C** (1986) 17;
L. Wolfenstein, *Phys. Rev.* **D 17** (1978) 2369
42. E. W. Kolb, M. S. Turner, *The Early Universe*, Addison-Wesley, New York, 1990

43. W. Fischler, G. F. Giudice, R. G. Leigh, S. Paban, Phys. Lett. **B 258** (1991) 45
44. W. Buchmüller, T. Yanagida, Phys. Lett. **B 302** (1993) 240
45. M. Flanz, E. A. Paschos, U. Sarkar, Phys. Lett. **B 345** (1995) 248; Phys. Lett. **B 384** (1996) 487 (E)
46. L. Covi, E. Roulet, F. Vissani, Phys. Lett. **B 384** (1996) 169
47. W. Buchmüller, M. Plümacher, Phys. Lett. **B 431** (1998) 354
48. For a discussion and references, see
A. Pilaftsis, Int. J. Mod. Phys. **A14** (1999) 1811
49. G. Lazarides, these proceedings
50. W. Buchmüller, M. Plümacher, Phys. Lett. **B 389** (1996) 73
51. M. Plümacher, Nucl. Phys. **B 530** (1998) 207
52. M. S. Turner, J. N. Fry, Phys. Rev. **D 24** (1981) 3341
53. W. Buchmüller, A. Jakovác, M. Plümacher, in preparation
54. H. Pagels, J. R. Primack, Phys. Rev. Lett. **48** (1982) 223
55. S. Weinberg, Phys. Rev. Lett. **48** (1982) 1303
56. M. D. Khlopov, A. D. Linde, Phys. Lett. **B 138** (1984) 265
57. J. Ellis, J. E. Kim, D. V. Nanopoulos, Phys. Lett. **B 145** (1984) 181
58. T. Moroi, H. Murayama, M. Yamaguchi, Phys. Lett. **B 303** (1993) 289
59. M. Bolz, W. Buchmüller, M. Plümacher, Phys. Lett. **B 443** (1998) 209
60. E. Braaten, T. C. Yuan, Phys. Rev. Lett. **66** (1991) 2183
61. M. Bolz, A. Brandenburg, W. Buchmüller, [hep-ph/0012052](#)
62. J. Ellis, G. B. Gelmini, J. L. Lopez, D. V. Nanopoulos, S. Sarkar, Nucl. Phys. **B 373** (1992) 399
63. M. Kawasaki, T. Moroi, Progr. Theor. Phys. **93** (1995) 879
64. E. Holtmann, M. Kawasaki, K. Kohri, T. Moroi, Phys. Rev. **D 60** (1999) 023506
65. T. Asaka, T. Yanagida, Phys. Lett. **B494** (2000) 297
66. T. Gherghetta, G. F. Giudice, A. Riotto, Phys. Lett. **B 446** (1999) 28
67. T. Asaka, K. Hamaguchi, K. Suzuki, Phys. Lett. **B490** (2000) 136
68. R. Kallosh, L. Kovman, A. Linde, A. van Proeyen, Phys. Rev. **D61** (2000) 103503
69. G. F. Giudice, A. Riotto, I. Tkachev, JHEP 9911 (1999) 036
70. J. Edsjö, P. Gondolo, Phys. Rev. **D 56** (1997) 1879